Interval parameter sensitivity analysis based on interval perturbation propagation and interval similarity operator

Yanlin Zhao[a,b], Xindong Li[b], Scott Cogan[c], Jiahui Zhao[b], Jianhong Yang[a,b]*, Debing Yang[a,b]*, Jingqi Shang[d], Bing Sun[e], Lechang Yang[a]

[a]School of Mechanical Engineering, University of Science and Technology Beijing, Beijing, China
[b]Shunde Innovation School, University of Science and Technology Beijing, Guangzhou, China
[c]Univ. Bourgogne Franche-Comt´e, CNRS/UFC/ENSMM/UTBM, Department of Applied Mechanics
[d]School of Astronautics, Beihang University, Beijing, China
[e]China Academy of Launch Vehicle Technology, Beijing, China
*Corresponding author: E-mail: yangjianhong@me.ustb.edu.cn, ustbydb@163.com

Abstract

An interval parameters sensitivity analysis is developed to quantify the impact of simulation model parameters on the model outputs. This sensitivity analysis contains two main steps the interval uncertainty propagation and the interval sensitivity index. The interval perturbation method is introduced to estimate the extreme bounds of model outputs according to the interval input parameters, which significantly reduces the computation cost of extensive Monte Carlo simulations. Since the output of the interval model are interval quantities, the traditional probabilistic sensitivity method and its sensitivity index is inappropriate as we only have the bounds of samples without inner data points. Hence, this work proposes an interval similarity operator based on the relative interval position operator, which is applicable to measure the variation of interval outputs. This interval sensitivity operator mainly quantifies the discrepancy between intervals based on six typical cases of the interval relative position. Finally, an academic case and a satellite structure case are analyzed to verify the feasibility and efficiency of the proposed method.

Keywords: Sensitivity analysis; interval uncertainty; interval sensitivity operator; interval relative position operator; interval perturbation method.

1 Introduction

A practical engineering model has to cope with various uncertainties existing in systems and structures. Uncertainties generally arise from the observed scattering of environmental conditions, lack of knowledge, inhomogeneity of materials, and measurement uncertainty. Those uncertainties are typically divided into two distinct forms, i.e., aleatory uncertainty and epistemic uncertainty (Kitahara et al. 2022). Meanwhile, non-deterministic analysis (Wang et al. 2011) has gained wide interest, and elaborate literature is available in this field. Uncertainty analysis can be generally classified into two categories of probabilistic and non-probabilistic techniques (Ql et al. 2021; Singh and Bhushan 2020). The interval model is one of the most representative non-probabilistic approaches, which quantifies the uncertainties by the bounds of datapoints. In this work, we mainly focus on the sensitivity analysis with interval uncertainties.

Sensitivity analysis (SA) has rapidly developed to quantify the impact of model parameters on outputs due to the growing complexity of mathematical models. One classical definition of sensitivity is "the study of how the uncertainty in the output of a model (numerical or otherwise) can be apportioned to different sources of uncertainty in the model inputs" (Andrea 2002), which is typically distinct from the uncertainty analysis. The importance of parameters is compared through ranked sensitivity indexes corresponding to each input parameter. The growth of uncertainty analysis has greatly promoted the development of sensitivity analysis.

The importance of sensitivity analysis is widely acknowledged. One object of sensitivity analysis is to identify the contributions of model inputs to the variation of the outputs, which is used as evidence for significant parameter selection before model calibration. For example, sensitivity analysis is generally distinguished between local methods (Ha 2018) and global methods (Sobol 2001). In the context of local methods, the changes in outputs are analyzed while one input parameter is changed, with the rest kept at reference values. Jacomel et al. (2021) presented a priori error estimates for local reliability-based sensitivity analysis. Achyut et al. (2022) proposed local sensitivity analysis by using an efficient approach called modified forward finite difference. Global sensitivity (Cheng et al. 2019) analysis captures the interaction effects among parameters when exploring the responses of the model by varying all inputs at the same time. Examples of global methods include the first-order sensitivity index of Sobol's method (Liu et al. 2019; Sobol 1993), the extended Fourier amplitude sensitivity test (Saltelli et al. 1999), the Morris screening method (Shin et al. 2013), the Multi-output support vector regression (M-SVR) (Cheng et al. 2019), and the distribution-based global sensitivity analysis (Lukáš 2022). When structures with large-scale parameters, it leads to the expensive computational cost issue due to quantifying the effects of inputs on the output response globally. A hybrid metamodel using the orthogonal constraints of radial basis function and sparse polynomial chaos expansions for the global sensitivity analysis of time-consuming models was developed (Wu et al. 2020).

Sensitivity analysis has been implemented in various areas, such as model Verification and Validation (V&V) (Eamon and Rais-Rohani 2008; Ehre et al. 2020; Papaioannou and Straub 2021; Suzana et al. 2022), structural optimization design (Eamon and Rais-Rohani 2008; Liu et al. 2019), structural reliability analysis (Ehre et al. 2020; Papaioannou and Straub 2021), mechanical property analysis of laminated plates (Longfei et al. 2012), and robust design in aerospace engineering (Dasari et al. 2020). However, most variance-based or moment-independent sensitivity analyses (Zhang et al. 2015; Zhou et al. 2014) involve evaluating partial derivatives of probabilistic model outputs at the nominal values of the input parameters, which should combine the sampling-based probabilistic methods and mathematical models to quantify uncertainties. In the case of a complex model with massive numbers of input variables, the sensitivity analysis from the probabilistic view is highly time-consuming.

In the context of non-probabilistic uncertainty quantification, the input parameters and output responses are both non-probabilistic. Traditional variance-based sensitivity analysis is inapplicable to the interval model due to the lack of probabilistic information on inputs and outputs. Recently, a prediction on the static response of structures with uncertain-but-bounded parameters based on the adjoint sensitivity analysis was developed, where the sensitivity analysis is implemented without considering the interval characteristics of uncertain parameters (Luo et al. 2020). It is necessary to consider interval uncertainties when sensitivity and uncertainty analysis is performed. Up to now, however, most sensitivity analysis methods and sensitivity coefficients are mainly established for probabilistic parameter selection, such as the Sobol sensitivity index (Sobol 1993), the total-effect index (Homma and Saltelli 1996), the Morris sensitivity index (Morris 1991)， and FAST sensitivity index (Mcrae et al. 1982). Sensitivity analysis is developed to provide information for the reliability-based design. Xiao and Huang et al. (2011) proposed a reliability sensitivity analysis method for the model with both epistemic and aleatory uncertainties using P-boxed. Bi et al. (2019) developed a stochastic sensitivity analysis with a novel sensitivity index based on the Bhattacharyya distance. Those research efforts have been made on sensitivity analysis when both hybrid epistemic and aleatory uncertainties. However, with the limitation of samples, the stochastic characteristics of parameters cannot be precisely determined. Besides, those mentioned probabilistic sensitivity coefficients for the stochastic models or models with hybrid uncertainties are not applicable to the model with purely non-probabilistic uncertainties. Hence, it is necessary to extend the sensitivity analysis to a wider application with only interval uncertainties. A novel sensitive coefficient based on the geometric interval quantification method is presented to quantify the parameter sensitivity in this paper.

The interval sensitivity analysis process relies on the accurate propagation of uncertainties in the form of intervals. However, the interval arithmetic operations are difficult to implement directly in uncertainty propagation. Interval analysis is introduced to estimate the interval outputs according to the interval inputs, which is named interval uncertainty propagation. Interval analysis is the basis of interval sensitivity, which predicts the interval output for estimating the sensitivity indices. Monte-Carlo simulation (Callens et al. 2022) is one of the typical uncertainty propagation methods which has been introduced into Sobol's sensitivity analysis. Interval analysis typically requires a global optimization procedure with Monte Carlo simulation to determine the interval bounds on the output side of a computational model. However, in the context of complex models in practice, massive Monte Carlo simulation brings excessive computation, sharply increasing the computation cost of sensitivity analysis. Some efficient interval propagation methods, such as advanced interval analysis (Fujita and Takewaki 2011), multivariate interval quantification approach based on the concept of the convex hull (Faes et al. 2019; Faes et al. 2017), Infor-gap uncertainty quantification models (Ben-Haim 2004), and some interval surrogate models (Fang et al. 2015; Khodaparast et al. 2011) are rapidly developed to reduce the computation cost. The interval perturbation methodology (Li et al. 2018; Wang and Qiu 2014), a representative interval propagation method, has some advantages over the Monte Carlo simulation, including lower computation cost because of calculating only by the information of a single point that allows the consideration of the complexity of structure. Therefore, this work introduces the interval perturbation propagation method to effectively estimate the output interval according to interval inputs.

A parameter sensitivity analysis method with a novel interval-based sensitivity metric is developed by introducing the interval propagation methodology in this work. The *interval similarity operator* (*ISO*) is employed as a sensitivity metric to measure the discrepancy between two interval model outputs corresponding to initial and changed interval parameters, respectively. This metric is developed for interval uncertainty quantification as it is computed only based on the extreme bounds of the interval without their inner data points. The interval perturbation method is adopted to estimate the bounds of model outputs to improve the computation effectiveness. The feasibility and accuracy of the proposed method is verified by two typical academic cases.

This work is organized as follows. Section 2 presents an overview of sensitivity analysis with interval uncertainties. Section 3 presents how to calculate the proposed interval-based sensitivity index. Section 4 illustrates the comprehensive framework of sensitivity analysis with interval uncertainties. Section 5 gives two study cases, i.e., an academic case and a more complex satellite case, to investigate the proposed method.

2 Background of sensitivity analysis for interval parameters

A finite element model or other complex black box models can be expressed as $\boldsymbol{F}(\cdot)$ as follows

$$\boldsymbol{f} = \boldsymbol{F}(\boldsymbol{\theta}) \tag{1}$$

where $\boldsymbol{f}$ is the model output. $\boldsymbol{F}$ represents a propagation function of the model system. $\boldsymbol{\theta}$ is the model parameters, where $\boldsymbol{\theta} = \{\theta_i\}, i = 1,2,3,\ldots,n$, and n is the number of model parameters.

The sensitivity index $\mathbf{S}$=$\{S_i\}$ of model parameter $\boldsymbol{\theta}$ is simply expressed as:

$$\mathbf{S} = \frac{\Delta \boldsymbol{f}}{\Delta \boldsymbol{\theta}} = \frac{\boldsymbol{F}(\boldsymbol{\theta}+\Delta\boldsymbol{\theta})-\boldsymbol{F}(\boldsymbol{\theta})}{\Delta \boldsymbol{\theta}} \tag{2}$$

where $\Delta\boldsymbol{\theta} = \{\Delta\theta_i\}$ represents the variation of parameter $\boldsymbol{\theta}$. $\Delta\boldsymbol{f} = \{\Delta f_j\}$ represents the variation of $\boldsymbol{f}$, where j=1, 2, …, m, m represents the dimensions of model output features.

In the context of a model with interval parameters $\boldsymbol{\theta^I}$, Eq. (1) can be given as

$$\boldsymbol{f^I} = \boldsymbol{F}\left(\boldsymbol{\theta^I}\right) \tag{3}$$

where $\boldsymbol{\theta^I} = \left\{\theta_i^I\right\}$ represents the interval parameters of model $\boldsymbol{F}$, and $\boldsymbol{f^I} = \left\{f_j^I\right\}$ are interval uncertainties. Then, the sensitivity index for interval parameters is accordingly converted as:

$$\mathbf{S}_{Int} = \frac{\partial \boldsymbol{f^I}}{\partial \Delta \boldsymbol{\theta}^I} = \frac{F(\boldsymbol{\theta^C}+\Delta\boldsymbol{\theta^I})-F(\boldsymbol{\theta^C}+\Delta\widehat{\boldsymbol{\theta}}\boldsymbol{^I})}{\Delta\boldsymbol{\theta^I}-\Delta\widehat{\boldsymbol{\theta}}\boldsymbol{^I}} \tag{4}$$

where $\Delta\widehat{\boldsymbol{\theta}}\boldsymbol{^I} = \left\{\Delta\hat{\theta}_i^I\right\}$ means the changed interval radius. It can be seen that $\Delta\boldsymbol{\theta^I}$ and $\Delta\widehat{\boldsymbol{\theta}}\boldsymbol{^I}$ is independent of the interval midpoints $\boldsymbol{\theta^C}$. We mainly focus on identifying the contributions of the slight change in model interval inputs to the variation of uncertainty degree of the outputs in this work.

For an interval variable $\boldsymbol{\theta^I}$, it can be determined by the extreme bounds $\underline{\boldsymbol{\theta}}$ and $\overline{\boldsymbol{\theta}}$ or by the inter center $\boldsymbol{\theta}^C$ and the interval radius $\Delta\boldsymbol{\theta}$, as follows:

$$\begin{aligned} \boldsymbol{\theta^I} &= [\boldsymbol{\theta}^c - \Delta\boldsymbol{\theta}, \boldsymbol{\theta}^c + \Delta\boldsymbol{\theta}] \\ &= \left[\underline{\boldsymbol{\theta}}, \overline{\boldsymbol{\theta}}\right] \end{aligned} \tag{5}$$

The fundamental operations of arithmetic for intervals (Moore 1996) are interpreted by two interval variables θ_1^I and θ_2^I, which is given as

$$\begin{cases} \theta_1^I + \theta_2^I = \left[\theta_1^l + \theta_2^l, \theta_1^u + \theta_2^u\right] \\ \theta_1^I - \theta_2^I = \left[\theta_1^l - \theta_2^u, \theta_1^u - \theta_2^l\right] \\ \theta_1^I \times \theta_2^I = [min\{\theta_1^l\theta_2^l, \theta_1^l\theta_2^u, \theta_1^u\theta_2^l, \theta_1^u\theta_2^u\}, max\{\theta_1^l\theta_2^l, \theta_1^l\theta_2^u, \theta_1^u\theta_2^l, \theta_1^u\theta_2^u\}] \\ \frac{\theta_1^I}{\theta_2^I} = \theta_1^I \times \left[\frac{1}{\theta_2^u}, \frac{1}{\theta_2^l}\right] \end{cases} \tag{6}$$

This work mainly focuses on the problem of local sensitivity analysis, which ignores the relationship between input parameters. The sensitivity analysis index $\mathbf{S}_{Int}$ is to quantify the impact of the change of interval parameters from $\boldsymbol{\theta^I}$ into $\boldsymbol{\theta^I} + \Delta\boldsymbol{\theta^I}$ on the model uncertainty output $\boldsymbol{f^I}$. Interval sensitivity analysis is simply illustrated in Fig. 1. We can find that for the sensitive interval parameters, once there is some variation in their boundaries, both the interval center and the interval radius of outputs significantly change. However, on the contrary, even if the insensitive interval parameters encounter large perturbations, it may cause a small impact on model outputs.

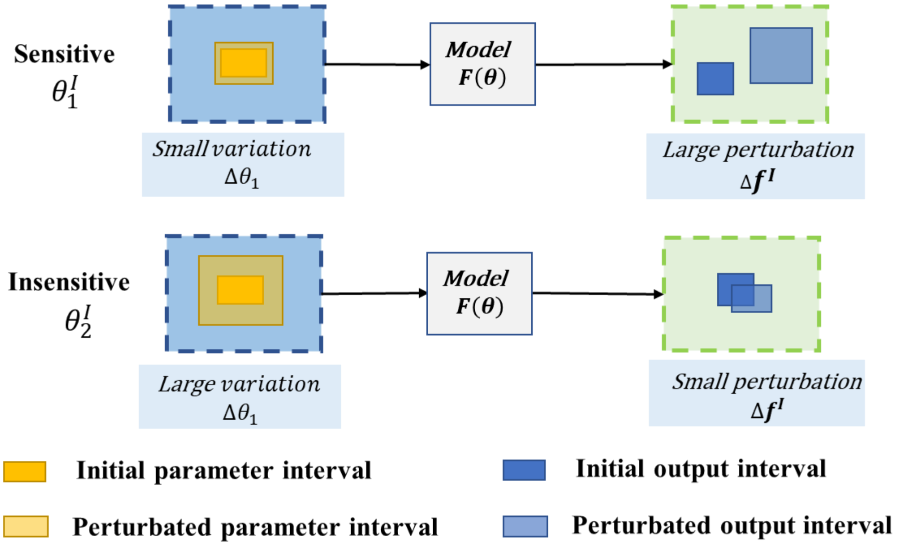

Fig. 1 Diagrammatic sketch for sensitivity analysis of interval parameters.

3 Interval perturbation FE method

In the context of a model containing interval uncertainties, Fig. 2 depicts the relationships among interval propagation, sensitivity analysis, and model updating, also called model calibration. The interval uncertainty propagation approach is investigated to determine the bounds of model outputs. The relative significance of interval parameters is assessed using sensitivity analysis. The model updating for sensitive inputs is applied to improve the accuracy of the simulation model. Interval propagation is regarded as a critical operator for both the sensitivity analysis and the model updating. The interval perturbation method (Zhao et al. 2018; Zhao et al. 2020), a typical interval propagation method, is investigated in this work.

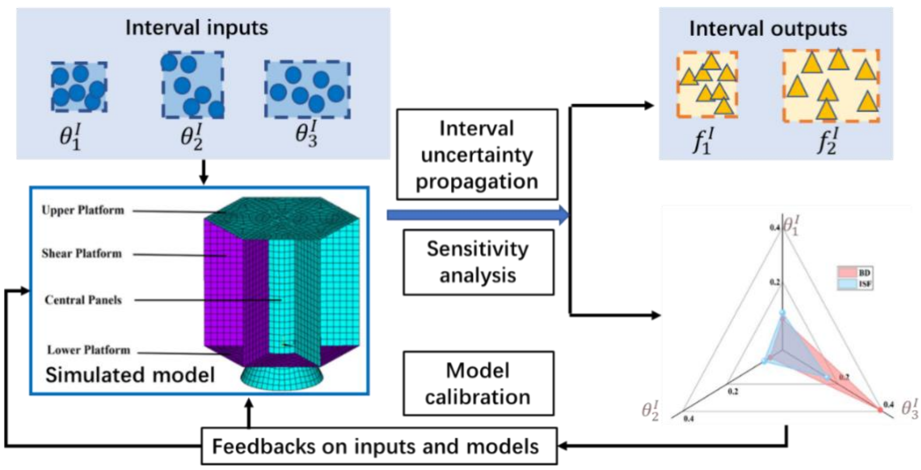

Fig. 2 The relationship between the sensitivity analysis, the interval uncertainty propagation, and the model calibration.

Interval uncertainties can be rewritten as

$$\boldsymbol{\theta}^{\boldsymbol{I}} = \{\theta_i^I\} = \{\theta^C + \Delta\theta^I\}_i, i = 1,2, \dots N \tag{7}$$

where $\theta_i^I = \theta_i^c + \Delta\theta_i^I = \theta_i^c + \Delta\theta_i \cdot \varepsilon_i^I$, and ε_i^I=[-1,1].

According to the perturbation method, the interval output $F(\boldsymbol{\theta}^{\boldsymbol{I}})$ can be given in a series mode as

$$\boldsymbol{F}(\boldsymbol{\theta}^{\boldsymbol{I}}) = \boldsymbol{F}(\varepsilon_i^I) = f_0 + \varepsilon_i^I f_1 + (\varepsilon_i^I)^2 f_1 + \ldots + (\varepsilon_i^I)^m f_m,\ i = 1,2, \ldots N \tag{8}$$

where m is the truncation order of the series. Based on the Taylor series expansion expanded at the middle point of the interval vector $\boldsymbol{\theta}^{\boldsymbol{I}}$, Eq. (8) can be transformed as

$$\begin{aligned}\boldsymbol{F}(\boldsymbol{\theta}^{\boldsymbol{I}}) = \boldsymbol{F}(\boldsymbol{\theta}^{\boldsymbol{C}}) &+ \sum_{p_1=1}^{N} \left.\frac{\partial \boldsymbol{F}(\boldsymbol{\theta})}{\partial \theta_{p_1}}\right|_{\theta_i^I=\theta^C, i\neq p_1} \cdot \Delta\theta_{p_1} \\ &+ \frac{1}{2}\sum_{p_1=1}^{N}\sum_{p_2=1}^{N} \left.\frac{\partial \boldsymbol{F}^2(\boldsymbol{\theta})}{\partial \theta_{p_1}\partial \theta_{p_2}}\right|_{\theta_i^I=\theta^C, i\neq p_1,p_2} \cdot \Delta\theta_{p_1}\Delta\theta_{p_2} + \cdots \\ &+ \frac{1}{m}\sum_{p_1=1}^{N}\cdots\sum_{p_m=1}^{N} \left.\frac{\partial \boldsymbol{F}^m(\boldsymbol{\theta})}{\partial \theta_{p_1}\ldots\partial \theta_{p_m}}\right|_{\theta_i^I=\theta^C, i\neq p_1,\ldots,p_m} \cdot \Delta\theta_{p_1}\ldots\Delta\theta_{p_m} + R\end{aligned} \tag{9}$$

Since the values of $\Delta\theta_{p_1} \cdot \Delta\theta_{p_2}, \ldots, \Delta\theta_{p_1} \cdot \ldots \cdot \Delta\theta_{p_m}$ in more than second-order form is very small, Eq.(9) can be approximated to a first-order form based on the interval algorithm, which is given as

$$\boldsymbol{F}(\boldsymbol{\theta}^{\boldsymbol{I}}) \cong \widehat{\boldsymbol{F}}(\boldsymbol{\theta}^{\boldsymbol{I}}) = \boldsymbol{F}(\boldsymbol{\theta}^{\boldsymbol{C}}) + \sum_{j=1}^{N} \left.\frac{\partial \boldsymbol{F}(\boldsymbol{\theta})}{\partial \theta_j}\right|_{\theta_i^I=\theta^C, i\neq j} \cdot \Delta\theta_j,\ j = 1,2, \ldots, N \tag{10}$$

Then, we can obtain the following equations that

$$\widehat{\boldsymbol{F}}(\boldsymbol{\theta}^{\boldsymbol{I}}) = \sum_{j=1}^{n}(\theta_j{}^c + \Delta\theta_j^I)F_i = \boldsymbol{F}(\boldsymbol{\theta}^{\boldsymbol{C}}) + \sum_{j=1}^{n} F_i \cdot \Delta\theta_j^I \tag{11}$$

where $F_i = \sum_{j=1}^{N} \left.\frac{\partial \boldsymbol{F}(\boldsymbol{\theta})}{\partial \theta_j}\right|_{\theta_i^I=\theta^C, i\neq j}$.

From Eq.(12), we can find that once we have the uncertain part of $\sum_{j=1}^{n} F_i \cdot \Delta\theta_j^I$, we can calculate the approximate bounds of the model output $\widehat{\boldsymbol{f}}^{\boldsymbol{I}} = \boldsymbol{F}(\boldsymbol{\theta}^{\boldsymbol{I}})$. The differential method is introduced to calculate the lower and upper bounds of the model output $\widehat{\boldsymbol{f}}^{\boldsymbol{I}}$, which is shown as

$$\begin{cases} \overline{\widehat{\boldsymbol{f}}} = F(\boldsymbol{\theta}^{\boldsymbol{c}}) + \sum_{j=1}^{N} \frac{\boldsymbol{F}(\theta_j^c + \delta\theta_j) - \boldsymbol{F}(\theta_j^c)}{\delta\theta_j} \Delta\theta_j \\ \underline{\widehat{\boldsymbol{f}}} = F(\boldsymbol{\theta}^{\boldsymbol{c}}) - \sum_{j=1}^{N} \frac{\boldsymbol{F}(\theta_j^c + \delta\theta_j) - \boldsymbol{F}(\theta_j^c)}{\delta\theta_j} \Delta\theta_j \end{cases} \tag{12}$$

where $\delta\theta_j$ is the minor variable of the interval variable θ_j.

4 Interval sensitivity analysis with *Interval Similarity Operator*

4.1 Interval Similarity Operator

In the context of local sensitivity analysis, for example, when the parameters are changed from $\boldsymbol{\theta}^{\boldsymbol{I}} = \{\theta_1^I, \theta_2^I, \ldots, \theta_n^I\}$ to $\widehat{\boldsymbol{\theta}}^{\boldsymbol{I}} = \{\hat{\theta}_1^I, \theta_2^I, \ldots, \theta_n^I\}$, namely θ_1^I becomes $\hat{\theta}_1^I$, the outputs are accordingly changed from the initial value of $\boldsymbol{f}^{\boldsymbol{I}} = \{f_j^I\}$ to the perturbed value of $\widehat{\boldsymbol{f}}^{\boldsymbol{I}} = \{\hat{f}_j^I\}$. It should be noted that although only one input parameter interval changes, all the output intervals are changed simultaneously. Zhao et al. (2022) proposed an uncertainty quantification metric of *interval similarity operator* (*ISO*) to address the issue of structural model updating. In this work, this metric is introduced to propose a novel sensitivity index to quantify the discrepancy between one-dimensional intervals $\boldsymbol{f^I}$ and $\boldsymbol{\hat{f}^I}$, reflecting the sensitivity of each input interval parameter.

Firstly, the *Interval Relative Position Operator* (*IRPO*) is utilized to measure the difference between two intervals based on the mathematical rule of interval length $L(\cdot)$, defined as follows:

$$L(f^I) = \overline{f} - \underline{f} \tag{15}$$

Two intervals $f^I = [\underline{f}, \overline{f}]$ and $\hat{f}^I = [\underline{\hat{f}}, \overline{\hat{f}}]$ are utilized to explain the proposed *Interval Similarity Operator*. Six typical positional relationships between intervals f^I and $\hat{f}^I$ are presented in Figure 3.

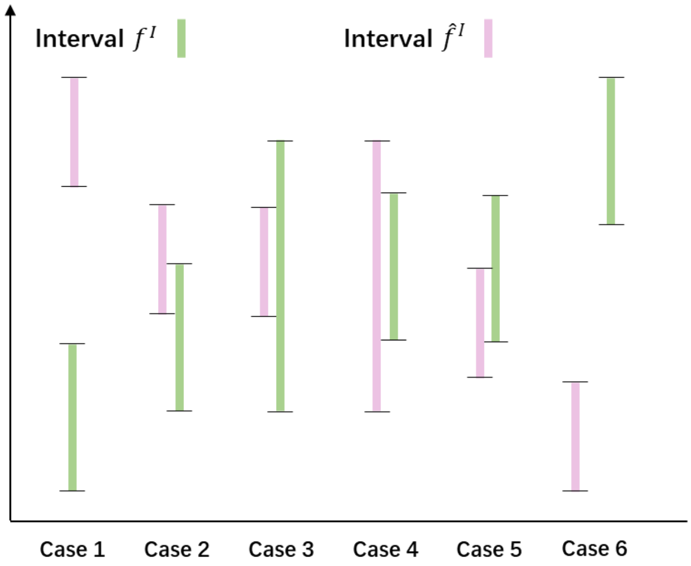

Fig. 3 Six interval relative positions.

The *IRPO* is calculated according to different overlap cases in Fig. 3, and its calculation rules are given as

$$IRPO(f^I, \hat{f}^I) = \begin{cases} \dfrac{\left(\overline{f} - \underline{\hat{f}}\right)}{max\{L(f^I), L(\hat{f}^I)\}} & Case\ 1{,}2 \\ \dfrac{\left(\overline{f} - \underline{f}\right)}{max\{L(f^I), L(\hat{f}^I)\}} & Case\ 3 \\ \dfrac{\left(\overline{\hat{f}} - \underline{\hat{f}}\right)}{max\{L(f^I), L(\hat{f}^I)\}} & Case\ 4 \\ \dfrac{\left(\overline{\hat{f}} - \underline{f}\right)}{max\{L(f^I), L(\hat{f}^I)\}} & Case\ 5{,}6 \end{cases} \tag{16}$$

where $max\{L(f^I), L(\hat{f}^I)\}$ represents the maximum interval length between f^I and $\hat{f}^I$.

For the cases 1 and 6, f^I and $\hat{f}^I$ have an overlapping space, and then the *IRPO* is negative. When the length of intervals f^I and $\hat{f}^I$ are infinite, the denominator of *IRPO* tends to zero. In cases 2-5, there is an overlap between f^I and $\hat{f}^I$, and the value of the IRPO is clearly positive and restrained to the range of (0,1). If both the position and the length of f^I is consistent with that of $\hat{f}^I$, $IRPO$ achieves its maximum value of 1. Hence the range of $IRPO$

is

$$IRPO(f^I, \hat{f}^I) \in (-\infty, 1] \tag{17}$$

Next, impose that the *IRPO* has a high gradient as the value moves close to one; we develop an *Interval Sensitivity Operator* based on the *IRPO* to quantify the similarity between two interval vectors concerning their geometric position and shape. The fundamental calculation rule of *ISO* is given by

$$ISO(\boldsymbol{f^I}, \boldsymbol{\hat{f}^I}) = mean\left(1 - \frac{1}{1+exp\{-IRPO\left(f_j^I, \hat{f}_j^I\right)\}}\right), j = 1,2, \ldots, m \tag{18}$$

where $mean(\cdot)$ represents the mean value of $(\cdot)$.

From Eq. (18), we can find that the value of *ISO* is limited within $(0, +\infty)$. A high gradient of Eq. (18) reflects the similarity between $\boldsymbol{f^I}$ and $\boldsymbol{\hat{f}^I}$. On the contrary, when ISO moves to the infinite positive, this means $\boldsymbol{f^I}$ is significantly different from $\boldsymbol{\hat{f}^I}$. In the context of sensitivity analysis, this implies that variations in parameter θ_i^I have a strong influence on the outputs $\boldsymbol{f^I}$.

According to Eq. (4), the proposed interval sensitivity index $\boldsymbol{S}$ based on *ISO* can be expressed as Eqs. (19)-(20). This index vector consists of a series of sensitive index variables $\{S_i, i = 1, \ldots, n\}$, and each variable S_i quantifies the sensitivity of parameter θ_i^I.

$$\boldsymbol{S} = \{S_i\}, i = 1, \ldots, n \tag{19}$$

$$S_i = \frac{\Delta \boldsymbol{f^I}}{\Delta \theta^I} = \frac{ISO(\boldsymbol{f^I}, \boldsymbol{\hat{f}^I})}{\Delta \theta_i^I} \tag{20}$$

We can rank the sensitivity index S_i in descending order to select the sensitive parameters. It should be noted that this proposed interval sensitivity index is calculated based on the boundaries of model outputs without any inner data points, which is especially appropriate for the model with pure interval uncertainties. Meanwhile, when there are stochastic uncertainties or hybrid stochastic and interval uncertainties in the model since the geometric position and range of model outputs can be measured through *ISO*, this index can be adopted for models with complicated uncertainties as well.

4.2 Framework of sensitivity analysis with interval uncertainties

This work belongs to the One-at-a-Time method (OAAT), so the problem of coupling between model parameters is not considered here. Besides, in contrast to the sensitivity analysis with stochastic uncertainties, this interval sensitivity analysis is performed with no hypothesis of probabilistic distributions. The objective is to quantify the variation of interval outputs $\boldsymbol{f^I} \rightarrow \boldsymbol{\hat{f}^I}$ caused by the change in the interval parameters $\theta_i^I \rightarrow \hat{\theta}_i^I$, such that the sequence of S_i represents the sensitivity of inputs $\boldsymbol{\theta^I}$.

The framework of the proposed sensitivity analysis method is illustrated in Fig. 4, which consists of three parts: (1) the major body, (2) the interval uncertainty propagation, and (3) the sensitivity index calculation. As mentioned above, the interval perturbation method is introduced to estimate model output intervals effectively. Then, the sensitivity index S_i corresponding to each parameter θ_i^I is accordingly calculated to measure the discrepancy between the initial interval output $\boldsymbol{f}^{\boldsymbol{I}}$ and the perturbated output $\hat{\boldsymbol{f}}^{\boldsymbol{I}}$. The major body contains a pre-determined initial and perturbed range of parameters, namely θ_i^I and $\hat{\theta}_i^I$. Finally, we rank the sensitivity index S_i in descending order. The detailed steps are illustrated as follows:

Step 1: The framework starts from a pre-determined range of the model parameters $\boldsymbol{\theta}^{\boldsymbol{I}} = \{\theta_1^I, \dots, \theta_n^I\}$ with its initial interval center $\boldsymbol{\theta}^{\boldsymbol{C}} = \{\theta_i^c\}$ and corresponding interval radius $\Delta\boldsymbol{\theta}^{\boldsymbol{I}} = \{\Delta\theta_i^I\}$. The initial interval θ^I represents the gross knowledge from engineering judgments.

Step 2: Select an interval parameter component θ_i^I and change its interval radius proportionally to model the small change of θ_i^I. Keep other interval parameter components unchanged. We finally obtain the interval perturbed parameter $\hat{\boldsymbol{\theta}}^{\boldsymbol{I}} = \{\theta_1^I, \dots, \hat{\theta}_i^I, \dots, \theta_n^I\}$.

Step 3: Estimate the initial model output interval $\boldsymbol{f}^{\boldsymbol{I}} = \{f_1^I, \dots, f_m^I\}$ and the perturbed output interval $\hat{\boldsymbol{f}}^{\boldsymbol{I}} = \{\hat{f}_1^I, \dots, \hat{f}_m^I\}$ through the interval perturbation method, which concerns the initial interval parameter $\boldsymbol{\theta}^{\boldsymbol{I}} = \{\theta_1^I, \dots, \theta_n^I\}$ and the perturbed interval parameter $\hat{\boldsymbol{\theta}}^{\boldsymbol{I}} = \{\hat{\theta}_1^I, \theta_2^I, \dots, \theta_n^I\}$, respectively.

Step 4: Calculate the *IRPO* and the *ISO* of $\boldsymbol{f}^{\boldsymbol{I}}$ and $\hat{\boldsymbol{f}}^{\boldsymbol{I}}$, and calculate the sensitivity value $\hat{S}_1$ corresponding to $\hat{\theta}_1^I$.

Step 5: Repeat Step 2-Step 4 n times to obtain a series of sensitivity indexes $\hat{S}_i, i = 1,2, \dots, n$ corresponding to interval parameters $\{\theta_1^I, \dots, \theta_n^I\}$.

Step 6: Sequence the value of $\hat{S}_i, i = 1,2, \dots, n$ in descending order to present the sensitivity of interval parameters $\{\theta_1^I, \dots, \theta_n^I\}$.

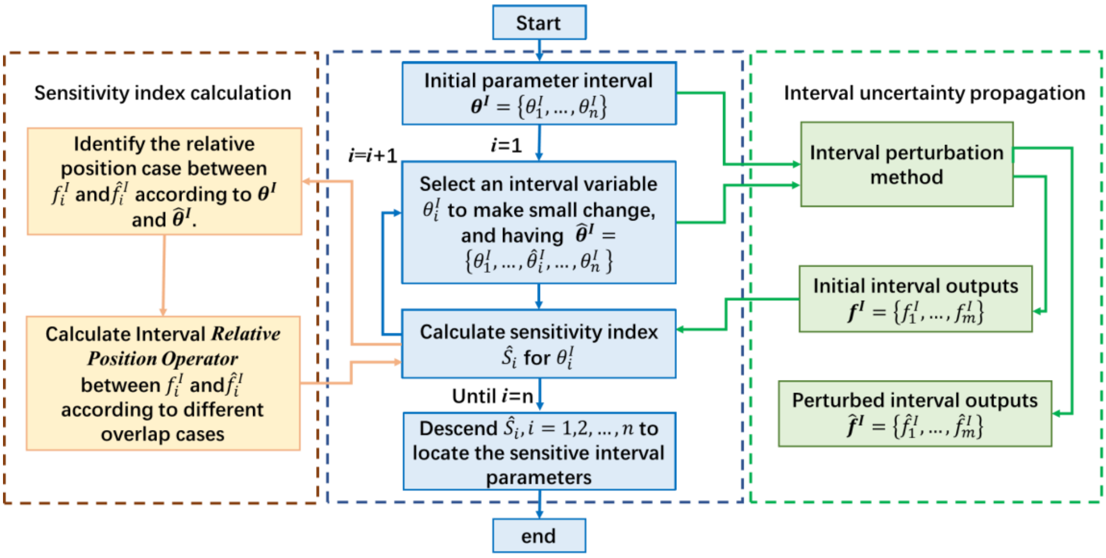

Fig. 4 Flowchart of sensitivity analysis for interval parameters.

6. Case studies

6.1 Case 1: Ishigami function

6.1.1 Problem description

A tutorial case study of the Ishigami function is presented in this section, which originated from Ref. (Ishigami and Homma 1990) and is analyzed by Ref. (Bi et al. 2019). The Ishigami function is a general example of sensitivity analysis, which is given as follows:

$$y(P) = \sin(p_1) + a\sin(p_2)^2 + bp_3^4\sin(p_1) \quad (21)$$

where $P = \{p_1, p_2, p_3\}$ is the input parameters; y is the output feature; *a* and *b* are constant coefficients with pre-determined values as Ref. (Marrel et al. 2008), a=7 and b=0.1.

Since Bi et al. (2019) mainly focus on the stochastic sensitivity analysis with both aleatory and epistemic uncertainties, the uncertainties p_{1-3} in Ref. (Bi et al. 2019) assumed that p_1 and p_2 are prescribed to follow the uniform distribution, and p_3 follows the Gaussian distribution. However, this uncertainty characteristic is inappropriate for the application of the proposed method because the determined distribution types of p_{1-3} belong to probabilistic uncertainties without any interval uncertainties.

In this case, p_{1-3} are defined as interval parameters, and according to Eq. (4), we assume that the lengths of interval radius $\boldsymbol{\Delta P}$ are changed 50% as presented in Table 1. For example, the initial length of Δp_1 is 0.8, which is changed to 0.4 in the perturbed interval $\hat{p}_1^I$, namely the interval of p_1^I is changed from [-2.4,-0.8] to [-2,-1.2]. Since this work is mainly about local sensitivity analysis, the other variables p_2^I and p_3^I of $\boldsymbol{P^I}$ are unchanged. By comparing the variation of the outputs caused by the initial and perturbed intervals of parameters, the sensitivity of each input can be identified.

Table 1 The initial and perturbed parameter intervals.

Parameters	p_1^I	p_2^I	p_3^I	Variation proportion ratio
Initial intervals $\boldsymbol{P^I}$	[-2.4,-0.8]	[-0.8,0.8]	[4.2,5.8]	50%
Perturbed intervals $\boldsymbol{\hat{P}^I}$	[-2,-1.2]	[-0.4,0.4]	[4.6,5.4]	50%

Since this work belongs to the problem of local sensitivity analysis, this interval sensitivity analysis aims to quantify the importance of each input according to how many intervals of uncertainty space of all outputs can be changed when the interval length of this initial input is proportionally increased, where the changed inputs are called perturbed inputs here. For this case, the perturbed interval parameters p_{1-3} are presented in Table 1. The objective of proportionally changing the interval radius $\Delta p^I = \{\Delta p_1^I, \Delta p_2^I, \Delta p_3^I\}$ to generate perturbed inputs with a radius of $\widehat{\Delta p}^I = \{\widehat{\Delta p}_1^I, \widehat{\Delta p}_2^I, \widehat{\Delta p}_3^I\}$ is illustrated in Figure 5, where the interval centers are completely fixed. The most intuitive manner is to measure how much the output interval space is changed to reflect the sensitivity of parameters. Hence the following operator to calculate the interval outputs according to p^I and $\hat{p}^I$. As the Ishigami function is simple, 5000 Monte Carlo simulations are conducted to estimate the initial interval outputs y^I and perturbed output $\hat{y}^I$.

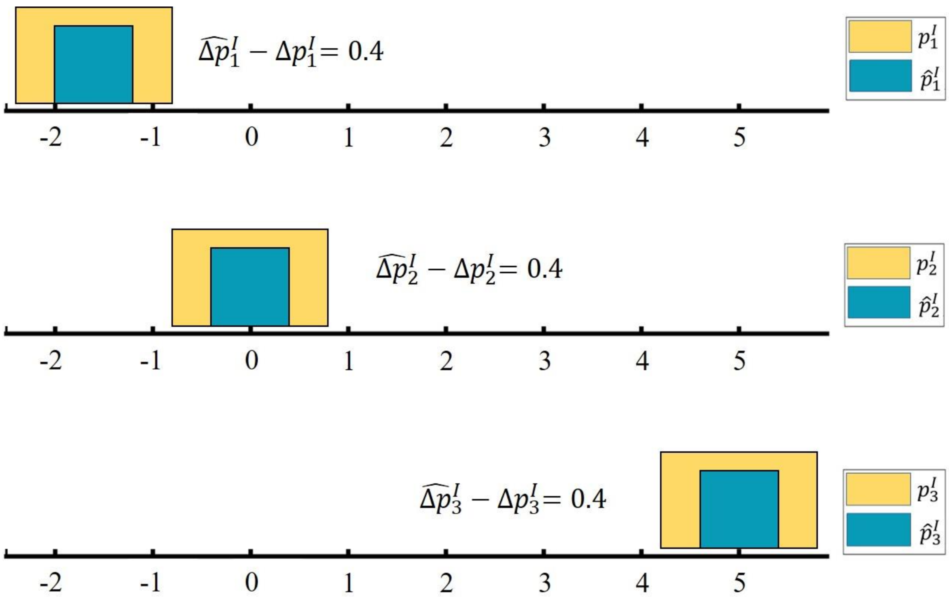

Fig. 5 Initial and perturbed input intervals.

Table 2 presents the initial output interval y^I calculated based on the initial parameter intervals p_1^I, p_2^I, and p_3^I. In the context of local sensitivity analysis, there are three perturbed interval output spaces corresponding to variations sequentially occurring in p_1^I, p_2^I, and p_3^I. The three perturbed interval outputs are given in Table 2. The output variability significantly reflects the degree of dispersion in the output uncertainty space, which is investigated in Figure 6. For example, the perturbed procedure is executed for an interval of $\hat{p}_1^I$ meanwhile, keeping the interval bounds of p_2^I, and p_3^I. Accordingly, the perturbed output $\hat{y}_{p1}^I$ is available. From Figure 6, it can be seen that the perturbation in p_3^I results in the most obvious changes in output, i.e. y^I to $\hat{y}_{p3}^I$, implying the p_3^I is sensitive to the outputs y^I.

Table 2 Initial and perturbed input intervals.

Initial parameters	Initial output y^I	Perturbed parameter orders	Perturbed output $\hat{y}^I$
		$\hat{p}_1^I, p_2^I, p_3^I$	$\hat{y}_{p1}^I$=[-113.07,-27.78]
p_1^I, p_2^I, p_3^I	y^I=[-111.55,-21.52]	$p_1^I, \hat{p}_2^I, p_3^I$	$\hat{y}_{p2}^I$=[-111.82,-22.04]
		$p_1^I, p_2^I, \hat{p}_3^I$	$\hat{y}_{p3}^I$=[-85.30,-29.65]

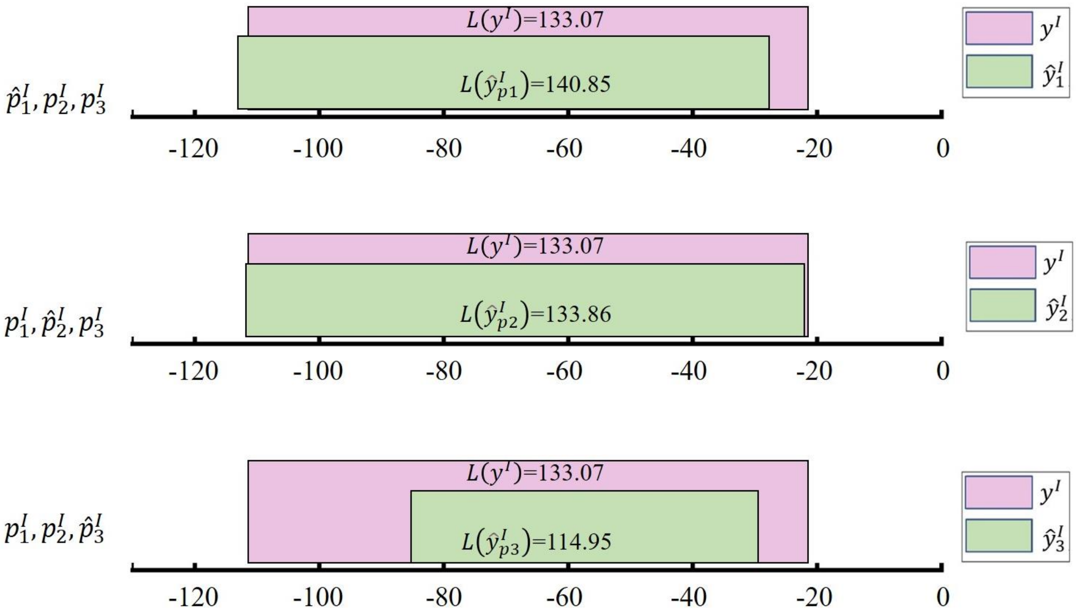

Fig. 6 Comparison between the initial and perturbated outputs intervals.

The *IRPO, ISO,* and comprehensive sensitivity index of p_1^I are evaluated according to Section 3. The same strategy is performed for p_2^I, and p_3^I, and their corresponding sensitivity indices are presented in Table 3. According to the determined input parameters, 5000 times Monte Carlo samples with the assumption of parameters following uniform distribution are performed to propagate the uncertainty from the inputs to the outputs, yielding 5000 data points bounded by the output intervals. Hence the sensitivity indices of Bhattacharyya distance in Ref. (Bi et al. 2019) can be adopted in this case, whose results are similar to those calculated by the proposed indices as shown in Figure 7.

Table 3 Sensitivity analysis of p_{1-3}.

Sensitivity index	$\hat{S}_{p_1}$	$\hat{S}_{p_2}$	$\hat{S}_{p_3}$	Sensitivity rank
Bhattacharyya distance Ref. (Bi et al. 2019)	0.02525	0.0055	0.228	$\hat{S}_{p_3} > \hat{S}_{p_1} > \hat{S}_{p_2}$
ISO	0.03475	0.003	0.20325	$\hat{S}_{p_3} > \hat{S}_{p_1} > \hat{S}_{p_2}$

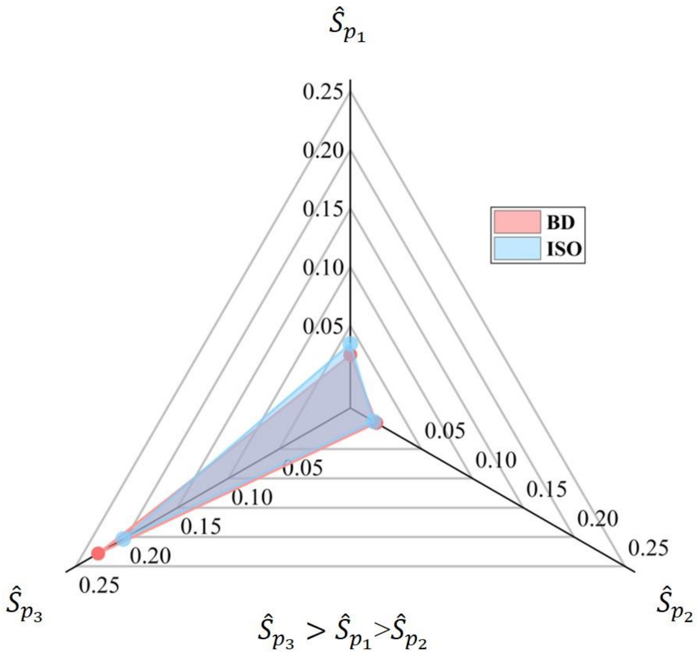

Fig. 7 Sensitivity analysis of p_1^I, p_2^I, and p_3^I

The sensitivity ranking is $\hat{S}_{p_3} > \hat{S}_{p_1} > \hat{S}_{p_2}$, and $\hat{S}_{p_1}$ and $\hat{S}_{p_2}$ are significantly smaller than $\hat{S}_{p_3}$, indicating that $\hat{S}_{p_3}$ is more sensitive than $\hat{S}_{p_1}$ and $\hat{S}_{p_2}$ from the point of view of interval uncertainty. Meanwhile, ISO_{p1} and ISO_{p2} are close to 0, implying a high geometric similarity between intervals y^I and $\hat{y}^I$.

It should be noted that the Bhattacharyya distance is calculated based on the distribution function of data, implying it is unable to deal with interval uncertainties. The proposed *ISO* is calculated only by the bounds of output intervals, which is reliable in engineering. Besides, the calculation time of the *ISO* is much less than that of the Bhattacharyya distance, which is proved by Fig. 8.

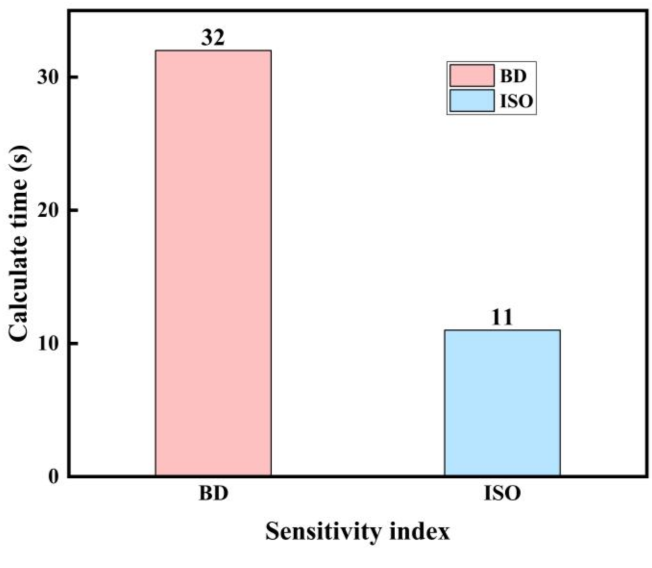

Fig. 8 Comparison of calculation time of the *ISO* and Bhattacharyya distance metrics.

6.1.2 Parameters with hybrid probabilistic and interval uncertainties

To assess the effectiveness of the proposed sensitivity analysis method, a published work on this Ishigami function, namely Ref. (Bi et al. 2019) is utilized herein as a reference to compare with the results of the current work. In Ref. (Bi et al. 2019), the parameters of the Ishigami function contain both hybrid probabilistic and interval uncertainties, which are expressed by the P-box technique. More complex uncertainty characteristics of the parameters are assigned as presented in Table 4, and correspondingly, the outputs y^{IR} are with hybrid stochastic and interval uncertainties. The P-box of an imprecise uniform distribution can be easily determined, i.e., the P-box of p_1 is enveloped by the CDFs of $\underline{p}_1 \sim \mathrm{U}(-4,2)$ and $\overline{p}_1 \sim \mathrm{U}(-3,3)$ as shown in Figure 9. The uncertainty of p_1 is controlled by the coefficients of a_1 and b_1 in **错误!未找到引用源。**, and the P-boxes of p_{2-3} can be determined by the uncertain coefficients of a_2, b_2, μ_3, and σ_3. A two-level procedure is proposed in Ref. (Bi et al. 2019) to calculate the P-boxes of outputs according to the input P-boxes. The Bhattacharyya distance is utilized to measure the discrepancy between the bounded CDF of the output P-box. For comparison, the proposed *ISO* is adopted to replace the Bhattacharyya distance for sensitivity analysis

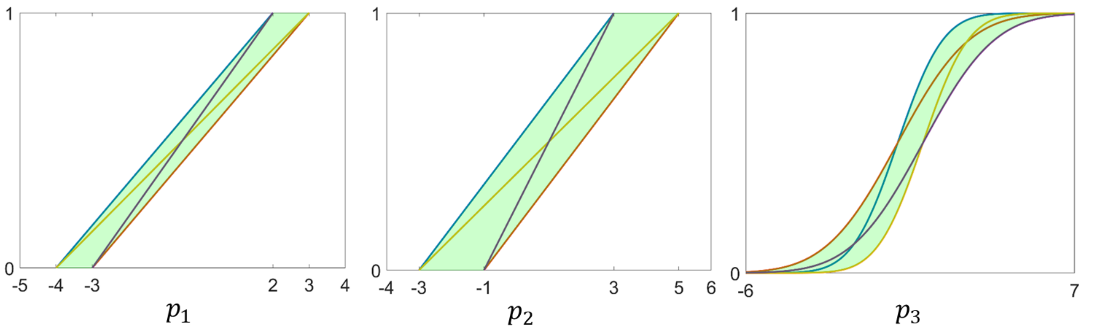

Fig. 9 The P-box of p_{1-3} in Ref. (Bi et al. 2019).

Table 4 Uncertainty characteristics of p_{1-3} in Ref. (Bi et al. 2019).

Parameters Ref. (Ishigami and Homma 1990)	Parameter probabilistic distribution	Uncertain coefficient
p_1	$p_1 \sim U(a_1^I, b_1)$	$a_1^I \in [-4.0,-3.0]; b_1^I \in [2.0,3.0]$
p_2	$p_2 \sim U(a_2^I, b_2)$	$a_2^I \in [-3.0,-1.0]; b_2^I \in [3.0,5.0]$
p_3	$p_3 \sim U(\mu_3^I, \sigma_3^2)$	$\mu_3^I \in [0.0,1.0]; \sigma_3^I \in [\sqrt{5},\sqrt{2}]$

To calculate the sensitivity of the parameter p_1, ten levels of interval a_1 and b_1 are investigated by assigning ten equidistant values within the intervals. The full factorial design results in 100 configurations of a_1 and b_1, and correspondingly 100 perturbated P-boxes of p_1 are obtained. Then 100 groups of perturbated P-boxes of outputs are simulated according to 100 groups of an interval variable $\{a_1^I, b_1^I\}_j$,j=1,..,100, respectively. To compare the uncertain space to give an explicit sensitivity ranking of p_{1-3}, the metrics of Bhattacharyya distance and

ISO are adopted to quantify the uncertainty space of the output P-box. Figure 10 presents one of the 100 perturbated P-boxes according to p_{1-3} in the form of CDFs, and Figure 11 gives specific data points of perturbated outputs. The sensitivity rank of parameters is evaluated based on the difference between the perturbed and original outputs concerning p_{1-3}.

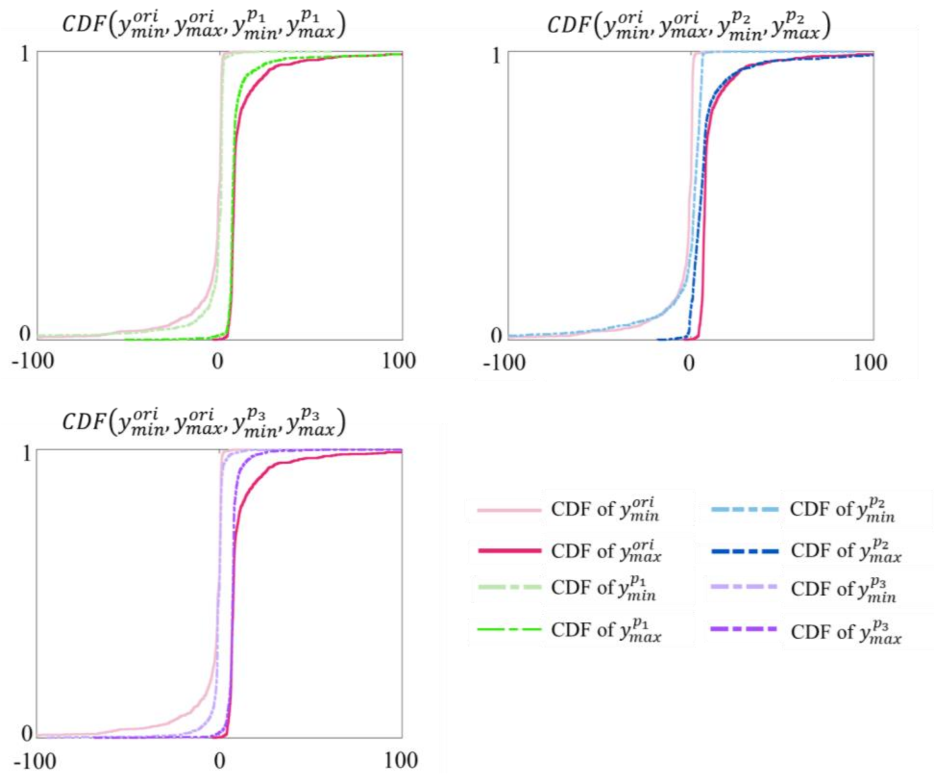

Fig. 10 Reduced output stochastic space when epistemic uncertainties of input parameters are reduced compared with the original P-box, which is calculated according to Ref. (Bi et al. 2019).

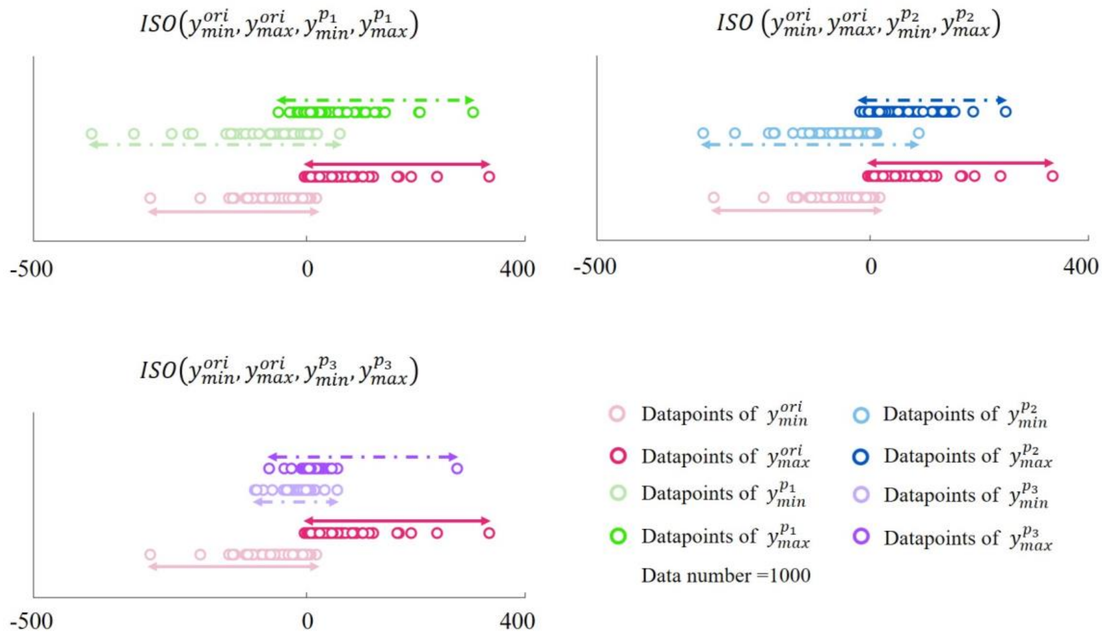

Fig. 11 Reduced output interval space when the epistemic uncertainties of input parameters

are reduced compared with the original P-box.

Figure 10 illustrates the sensitivity rank rule of Ref. (Bi et al. 2019), where the reduced uncertainty space of output is measured from the view of CDF. Figure 11 investigates the variation between the original and perturbed output uncertainty space by applying the interval concept. It is difficult to rank the parameter sensitivity with manual observation, but it is easy to directly tell the sensitivity rank through an interval observation mode, as shown in Figs 10-11. Since those uncertain data points are quantified by different uncertainty quantification tools, the results of sensitivity rank are inconsistent, as shown in Table 5 and Fig.12.

Table 5 Uncertainty characteristics of p_{1-3}.

Rank	Results according to different indices	
	$\hat{S}_{ISO}$	$\hat{S}_{BD}$ in Ref. (Bi et al. 2019)
1	$\hat{S}_{p_3}$	$\hat{S}_{p_2}$
2	$\hat{S}_{p_1}$	$\hat{S}_{p_1}$
3	$\hat{S}_{p_2}$	$\hat{S}_{p_3}$

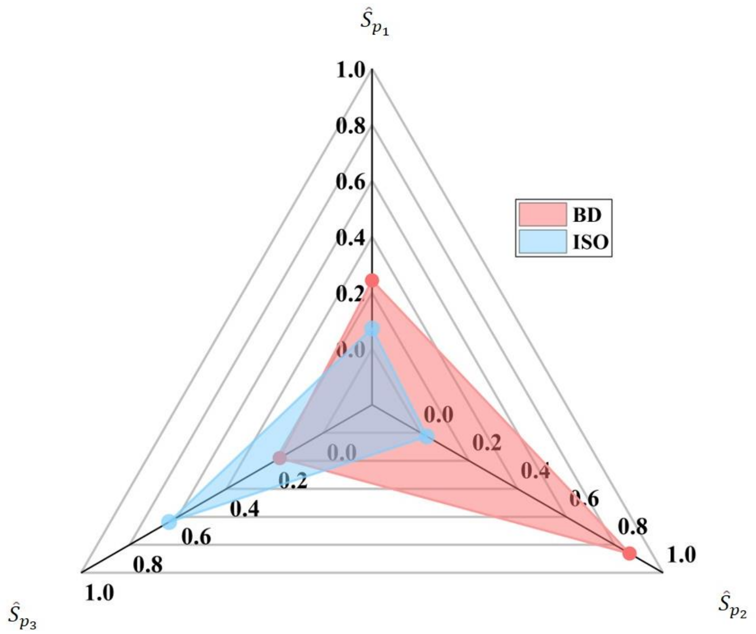

Fig. 12 Sensitivity analysis comparison with respect to the metrics of *ISO* and Bhattacharyya distance.

From the point of view of the interval concept, the uncertain output space of p_3 is changed most obviously compared with the original one, where the subjective judgment consists of the objective calculation results calculated by *ISO*. The ranks calculated by *ISO* differ from that of Ref. (Bi et al. 2019). This is because the interval is mainly affected by the extreme data points, while the CDF is calculated according to the dispersion of the datapoints. The sensitivity rank computed by interval uncertainty quantification of *ISO* is credible. This is because we mainly focus on the low-probability tail risk, which occurs when the model outputs are extremely large or small in engineering practice. It can be found that the change in data from the probabilistic point of view cannot imply a significant change in data from the interval point of view.

6.2 Case 2: Satellite FE model

This case of a satellite model is derived from Ref. (Zhang et al, 2019), which is utilized for model calibration analysis. Here, this model is analyzed to demonstrate the performance of the *ISO* metric within the proposed sensitivity analysis. The FE model of the satellite is presented in Figure 13, and this model consists of the upper platform, the shear platform, the central panels, and the lower platform.

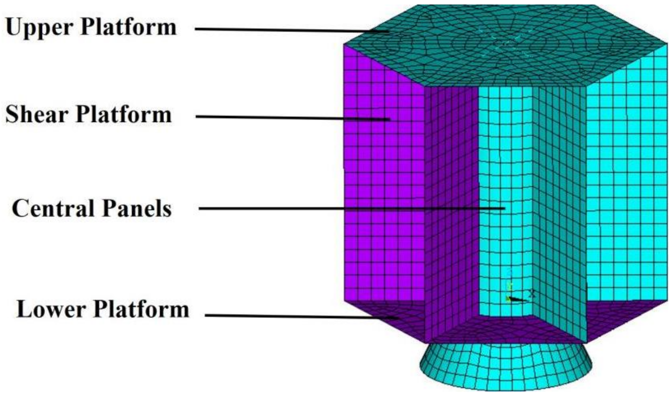

Fig. 13 Finite element model of the satellite.

6.2.1 Interval uncertainties propagation

In this satellite FE model, the Elastic modulus of the FE model θ_1 is 7.0×10^{10}pa, the density θ_2 is 2.7×10^{3}kg·m^{-3}, and the thickness of the lower platform θ_4 is 1mm. Some parameters of this FE model are assumed to be interval as given in Table 6. The first two eigenfrequency intervals f_1^I and f_2^I are regarded as the model output features.

Table 6 Satellite parameter table

Parameters		Interval centers	Interval radius
θ_3^I	The thickness of the central panel	2 (mm)	0.2 (mm)
θ_5^I	The thickness of the shear platform	3 (mm)	0.2 (mm)
θ_6^I	The thickness of the upper platform	2 (mm)	0.2 (mm)

Since it is time-consuming to calculate the FE model of the satellite structure, the interval perturbation method is adopted to estimate the interval outputs efficiently. 10000 Monte Carlo simulations are conducted to estimate f_1^I and f_2^I. The results of the two methods are presented in Fig. 14 and Table 7. It can be found that the bounds calculated by the perturbated method are consistent with that of MC simulation, demonstrating the accuracy of the interval perturbation method. Besides, the calculation time of MC simulations is 85960s, while that of the interval perturbation method is about 240s, as shown in Fig. 15. This illustrates the effectiveness of interval perturbation method when coping with the problem of interval propagation.

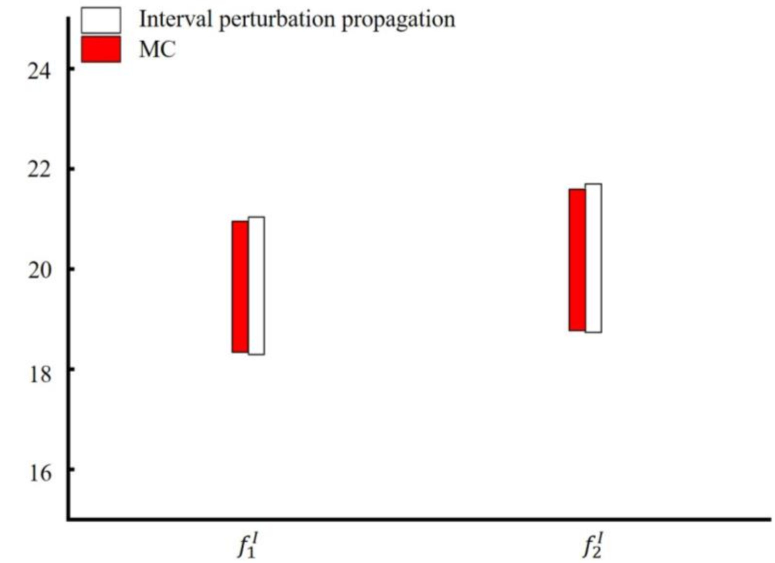

Fig. 14 Interval of f_1^I and f_2^I calculated by MCS and the interval perturbation method.

Table 7 Interval perturbation method

Parameters	MC simulation	Interval perturbation method	Relative error
f_1^I	[18.33,20.94]	[18.29, 21.04]	[0.21%, 0.47%]
f_2^I	[18.78, 21.6]	[18.74, 21.7]	[0.21%, 0.46%]

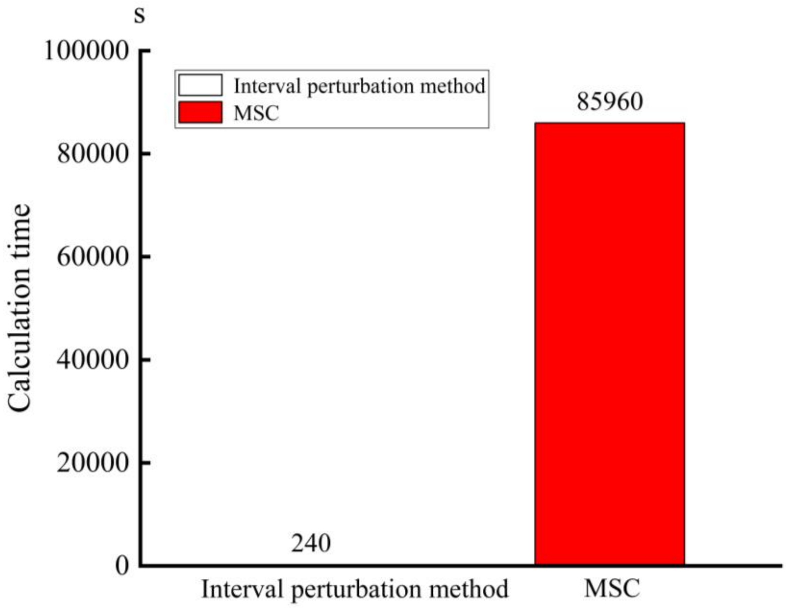

Fig. 15 Comparison of calculation time between MCS and the interval perturbation method.

6.2.2 Sensitivity analysis of θ_3^I, θ_5^I and θ_6^I

A sensitivity analysis is executed for some interval parameters of the θ_3^I, θ_5^I and θ_6^I. Proportional changes in the interval radius $\Delta\theta^I=\{\Delta\theta_3^I,\Delta\theta_5^I,\Delta\theta_6^I\}$ generate input intervals with the perturbed radius of $\widehat{\Delta\theta}^I=\{\widehat{\Delta\theta}_3^I,\widehat{\Delta\theta}_5^I,\widehat{\Delta\theta}_6^I\}$, where the interval centers are completely fixed. Figure 16 intuitively presents the changed interval inputs, and Table 8 lists the initial parameter interval θ^I and the perturbed parameter interval $\hat{\theta}^I$.

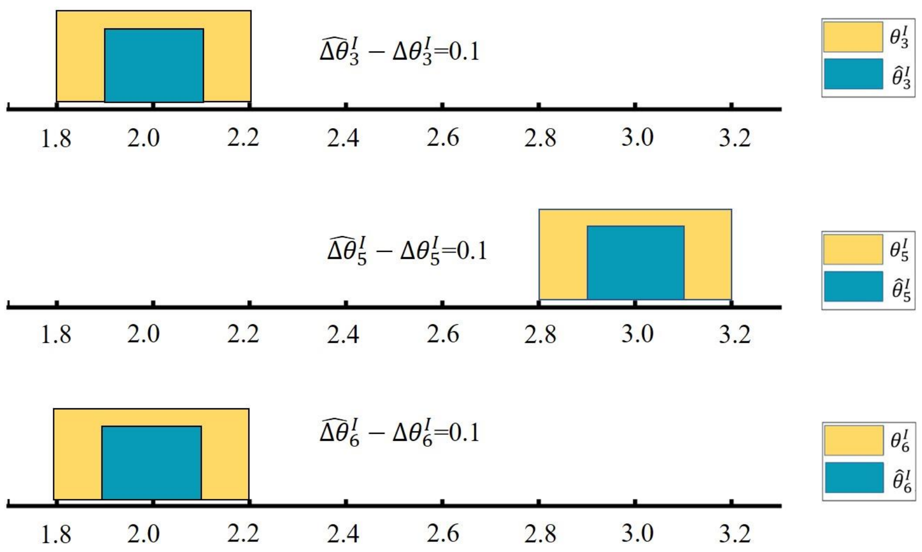

Fig. 16 Comparison between initial and perturbed input intervals.

Table 8 The initial and perturbed intervals of θ_3^I, θ_5^I and θ_6^I

Parameters	θ^I	$\hat{\theta}^I$	Variation proportion ratio of interval radius
θ_3^I	[1.8,2.2]	[1.9,2.1]	50%
θ_5^I	[2.8,3.2]	[2.9,3.1]	50%
θ_6^I	[1.8,2.2]	[1.9,2.1]	50%

The initial output intervals f_1^I and f_2^I are calculated according to the initial parameters θ_3^I, θ_5^I and θ_6^I. Next, the sensitivity framework in Section 4 is implemented to rank the sensitivity of input parameters. Three perturbed interval output spaces $\hat{\theta}^I$ are listed in Table 9 respective to the parameter perturbed sequentially. The initial and perturbed output intervals of f_1^I and f_2^I are shown in Figs. 17 -18, respectively.

Table 9 Sensitivity analysis for θ_3^I, θ_5^I and θ_6^I

Parameters	Perturbated $\hat{f}^I$	Initial f^I	$\hat{S}_{\theta_i}$	Sensitivity rank
$\hat{\theta}_3^I, \theta_5^I, \theta_6^I$	$\hat{f}_1^I = [18.50,20.83]$ $\hat{f}_2^I = [18.97,21.47]$		3.004	
$\theta_3^I, \hat{\theta}_5^I, \theta_6^I$	$\hat{f}_1^I = [18.71,20.62]$ $\hat{f}_2^I = [19.19,21.26]$	f_1^I =[18.29,21.04] f_2^I =[18.74,21.70]	3.326	$\hat{S}_{\theta_5} > \hat{S}_{\theta_3} > \hat{S}_{\theta_6}$
$\theta_3^I, \theta_5^I, \hat{\theta}_6^I$	$\hat{f}_1^I = [18.35,20.98]$ $\hat{f}_2^I = [18.81,21.64]$		2.772	

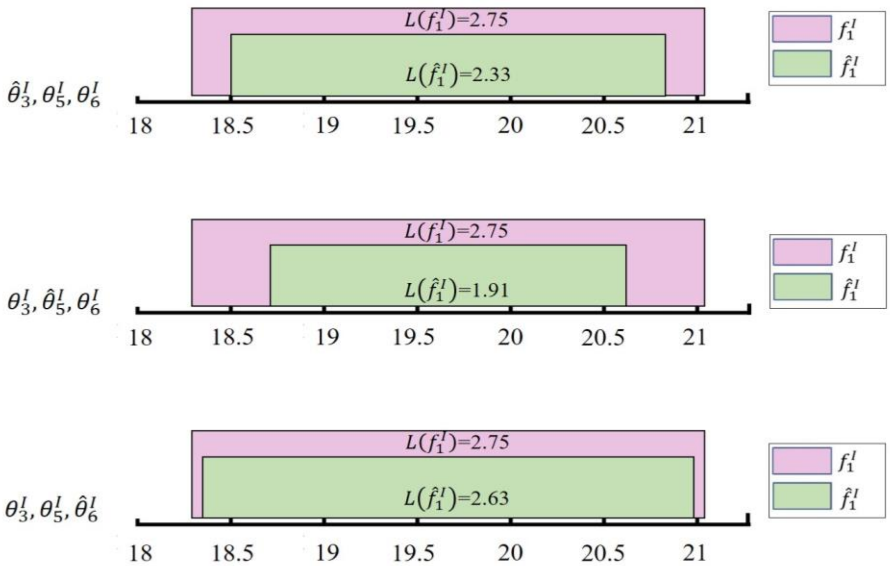

Fig. 17 Initial and perturbated output intervals of f_1^I

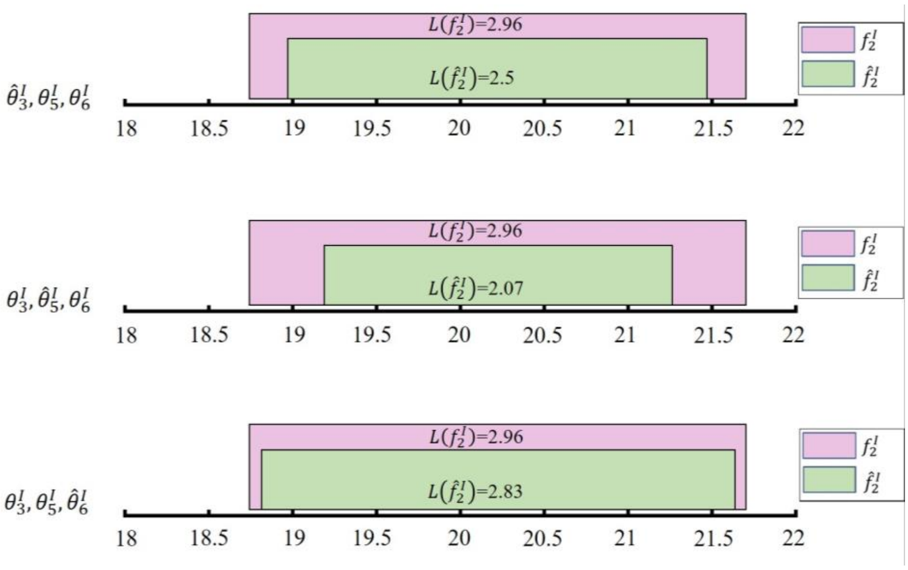

Fig. 18 Initial and perturbed output intervals of f_2^I.

From Figs. 17-18, we can find that the variations between the initial and perturbed outputs space of $\hat{\theta}_5^I$ are the largest, which reveals the impact of the model input interval parameter θ_5^I, namely the thickness of the shear platform on the model output intervals f_1^I and f_2^I is significant. On the contrary, θ_6^I is the least important parameter. The last column of Table 9 presents the ranking results of the current work, namely $\theta_5 > \theta_3 > \theta_6$, according to the proposed sensitivity index, which is visualized in Fig. 19. The sensitivity ranks imply that the interval uncertainty of shear platform thickness θ_5 significantly impacts the primary model natural frequencies of the satellite model.

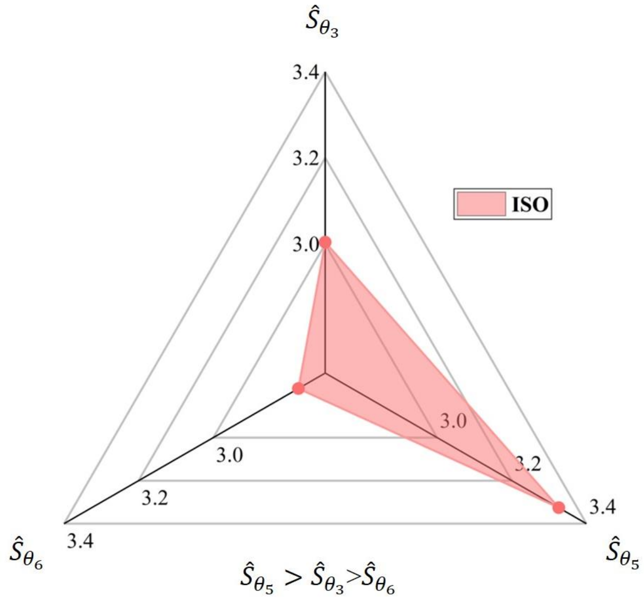

Fig. 19 Sensitivity order of θ_3^I, θ_5^I, and θ_6^I

6.2.3 Sensitivity analysis for model with multiple parameters and multiple outputs

In this section, the parameters θ_1, θ_2, and θ_4 are assumed to be intervals, and the first eigenfrequency to the eighth eigenfrequency f_{1-8}^I are investigated as multiple output features. The proposed sensitivity analysis is performed for six parameters θ_{1-6}^I, and the initial and perturbed intervals of parameters are presented in Table 10.

Table 10 The initial and perturbated intervals of θ_1^I to θ_6^I

Parameters	θ^I	$\hat{\theta}^I$	Variation proportion ratio of interval radius
θ_1^I	[6.8,7.2]	[6.9,7.1]	50%
θ_2^I	[2.5,2.9]	[2.6,2.8]	50%
θ_3^I	[1.8,2.2]	[1.9,2.1]	50%
θ_4^I	[0.8,0.2]	[0.9,1.1]	50%
θ_5^I	[2.8,3.2]	[2.9,3.1]	50%
θ_6^I	[1.8,2.2]	[1.9,2.1]	50%

We calculate the sensitivity indexes with respect to each parameter, and finally rank them as given in Table 11 and Fig 20. θ_4^I, the lower platform of the satellite model, is the most sensitive parameter among those six interval parameters, and θ_6^I, the thickness of the upper platform is the most not sensitive parameter. Besides, it should be noted that the rank of θ_3^I, θ_5^I, and θ_6^I in this case is consistent with that in Section 6.2.2, while with the different sensitivity index value. This is because the dimensions of outputs are increased from 3 to 8. For multiple outputs, the sensitivity of parameters is not changed in this Satellite FE model, which illustrates the stability of the proposed sensitivity analysis method.

Table 11 Sensitivity analysis for θ_{1-6}^{I}.

Parameters	$\hat{S}_{\theta_i}$ with *ISO*	Sensitivity rank
θ_1^I	2.844	$\hat{S}_{\theta_4} > \hat{S}_{\theta_2} > \hat{S}_{\theta_5} > \hat{S}_{\theta_3} > \hat{S}_{\theta_1} > \hat{S}_{\theta_6}$
θ_2^I	3.033	
θ_3^I	2.880	
θ_4^I	3.206	
θ_5^I	2.951	
θ_6^I	2.836	

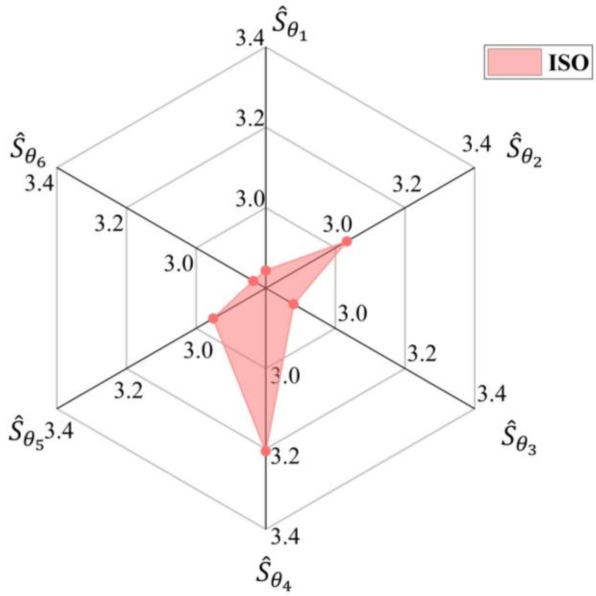

$\hat{S}_{\theta_4} > \hat{S}_{\theta_2} > \hat{S}_{\theta_5} > \hat{S}_{\theta_3} > \hat{S}_{\theta_1} > \hat{S}_{\theta_6}$

Fig. 20 Sensitivity order of θ_{1-6}^{I}

Since the proposed method is a local sensitivity analysis method, we can determine the sensitivity of each output feature of f_1^I to f_8^I to each parameter based on the sensitivity index with *ISO*. For example, Fig. 21 presents the initial and perturbed intervals of f_1^I to f_8^I concerning the most sensitive parameter θ_4^I. We can observe that the variations between the f_8^I and $\hat{f}_8^I$ cased by the changes of θ_4^I are apparent, and the value of *ISO* between f_8^I and $\hat{f}_8^I$ is 0.3568. Meanwhile, the most stable parameter of θ_6^I, the changes in θ_6^I lead to slight changes in outputs f_1^I to f_8^I as shown in Fig. 22. The proposed method not only can order the sensitivity of interval parameters but also can measure the changes of each interval output features.

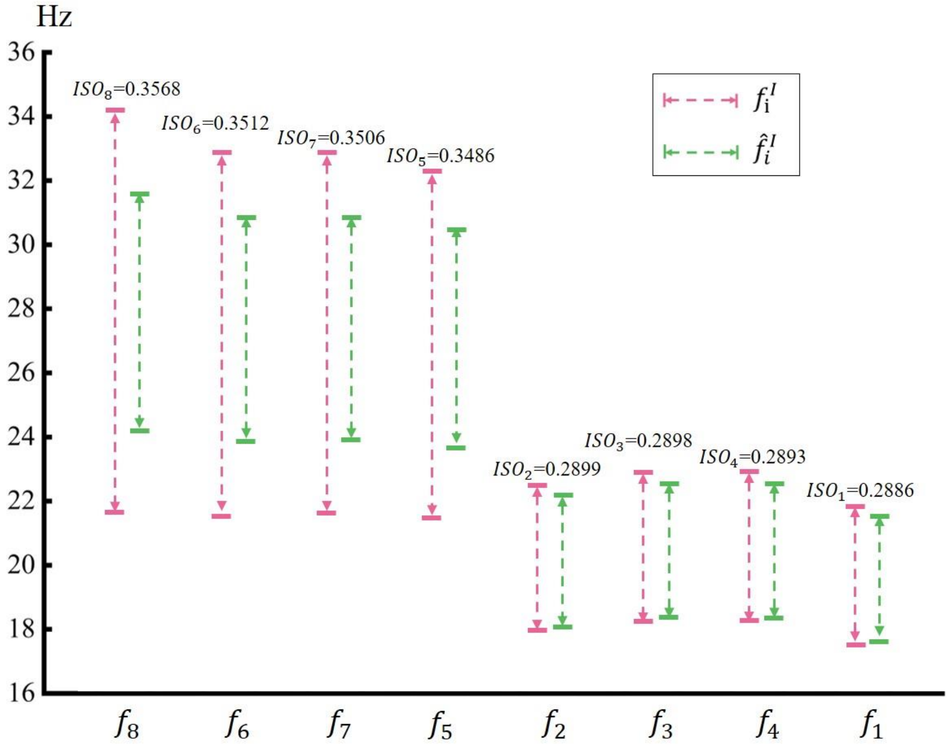

Fig. 21 The variation of f_1^I to f_8^I results from the changes of θ_4^I

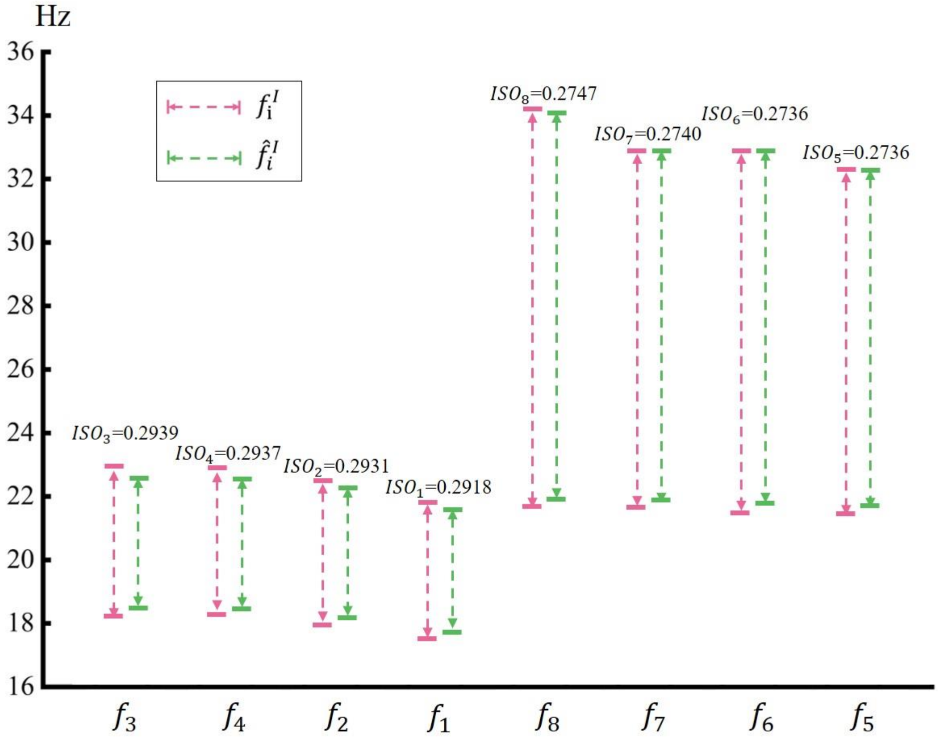

Fig. 22 The variation of f_1^I to f_8^I results from the changes of θ_6^I

In order to examine the potential impact of variation proportion ratio of parameter interval radius on the sensitivity of parameters, the sensitivity ranks for θ_1^I to θ_6^I corresponding to different variation of the parameter interval radius are shown in Table 12 and Fig. 23.

Table 12 TSensitivity ranks according to different variation proportion ratio of interval radius.

Variation proportion ratio of interval radius	Sensitivity ranks of θ_1^I - θ_6^I
10%	$\hat{S}_{\theta_4} > \hat{S}_{\theta_2} > \hat{S}_{\theta_5} > \hat{S}_{\theta_6} > \hat{S}_{\theta_3} > \hat{S}_{\theta_1}$
20%	$\hat{S}_{\theta_4} > \hat{S}_{\theta_5} > \hat{S}_{\theta_2} > \hat{S}_{\theta_1} > \hat{S}_{\theta_3} > \hat{S}_{\theta_6}$
30%	$\hat{S}_{\theta_4} > \hat{S}_{\theta_2} > \hat{S}_{\theta_5} > \hat{S}_{\theta_3} > \hat{S}_{\theta_1} > \hat{S}_{\theta_6}$
40%	$\hat{S}_{\theta_4} > \hat{S}_{\theta_5} > \hat{S}_{\theta_2} > \hat{S}_{\theta_6} > \hat{S}_{\theta_3} > \hat{S}_{\theta_1}$
50%	$\hat{S}_{\theta_4} > \hat{S}_{\theta_2} > \hat{S}_{\theta_5} > \hat{S}_{\theta_3} > \hat{S}_{\theta_1} > \hat{S}_{\theta_6}$
60%	$\hat{S}_{\theta_4} > \hat{S}_{\theta_5} > \hat{S}_{\theta_2} > \hat{S}_{\theta_3} > \hat{S}_{\theta_1} > \hat{S}_{\theta_6}$

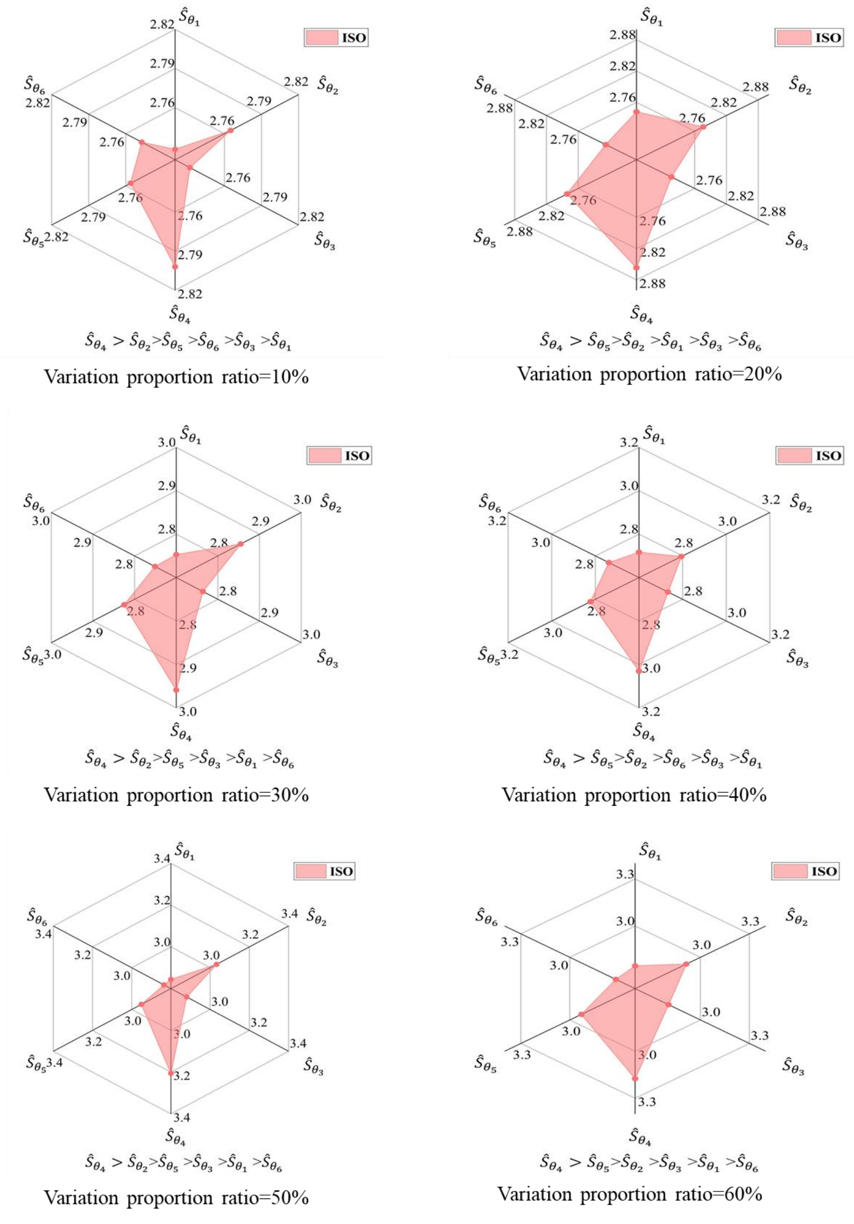

Fig. 23 Sensitivity ranks of θ_1^I - θ_6^I correpongding to different variation proportion ratio of interval radius.

We can find that as the variation proportion ratio of the interval radius increases from 10% to 60%, the sensitivity ranks of parameters experience slight changes. Of notable significance is parameter θ_4^I, which represents the thickness of the lower platform, as it consistently maintains the first order rank in influencing output features, regardless of the variation of the parameter interval radius. Conversely, uncertainties surrounding parameter θ_6^I, which denotes the thickness of the upper platform, have minimal impact on output uncertainty and rank towards the end of the sensitivity order. Henc, it is recommended to pay more attention to the thickness of the lower platform, and it may be more beneficial to focus on adjusting and optimizing parameter θ_4^I in order to achieve desired output results.

7 Conclusion

An exhaustive interval sensitivity analysis method based on the interval perturbation method and *interval similarity operator* is developed. In this interval sensitivity analysis framework, the *ISO* metric is adopted to quantify the discrepancy between two intervals based on the interval geometric position and the interval bounds without requiring inner interval samples. This metric can rank different sensitivity analysis frameworks, e.g. interval sensitivity analysis and sensitivity analysis with hybrid stochastic and interval uncertainties, which is illustrated by the tutorial case of the Ishigami function. The interval perturbation method is introduced for interval uncertainty propagation, which has the advantage of not requiring abundant FE simulation to estimate precise extreme bounds of interval outputs. It is a significant benefit for sensitivity analysis in the presence of practical engineering structures. The feasibility and effectiveness of this proposed interval sensitivity analysis algorithm are verified by two numerical examples of the classical Ishigami function and the satellite example. Further development for interval analysis includes the applications for nonlinearity systems, the consideration of the inner relationship between multi-dimensional outputs, and the hybrid stochastic and interval uncertainties propagation.

Declaration of Competing Interest

The authors declare that they have no known competing financial interests or personal relationships that could have appeared to influence the work reported in this paper.

Replication of results: All modeling parameters are given in the case, and the corresponding finite element model can be obtained according to the case modeling. The presented results are produced using our in-house code surrogate-based optimization and sensitivity analysis. The code and data for producing the presented results will be made available by request. The relevant codes for the algorithms could be available on request by emailing the first author. The authors wish to withhold the source code for commercialization purposes. This includes the finite strain elastoplastic analysis code implementing the finite strain elastoplastic analysis and adjoint sensitivity analysis.

Acknowledgments: The authors gratefully acknowledge the support of the Postdoctoral Research Foundation of Shunde Innovation School, University of Science and Technology Beijing (2021BH012), the Fundamental Technical Project (JSZL2020203B001), the International Communication Foundation of the University of Science and Technology Beijing (QNXM20220028), the National Natural Science Foundation of China (52005032 and 72271025), and the Guangdong Basic and Applied Basic Research Foundation(2022A1515110276).

References

Achyut P, Subham G, Mishal T, Mulani, SB, Walters, RW (2022) Higher-order Taylor series expansion for uncertainty quantification with efficient local sensitivity. Aerospace Science and Technology, 126.

Andrea S (2002) Sensitivity analysis for importance assessment. Risk analysis: an official publication of the Society for Risk Analysis, 22(3).

Ben-Haim Y (2004) Uncertainty, probability and information-gaps. Reliability Engineering and System Safety, 85(1/3), 249-266.

Bi SF, Broggi M, Wei PF, Beer M (2019) The Bhattacharyya distance: Enriching the P-box in stochastic sensitivity analysis. Mechanical Systems and Signal Processing, 129.

Cheng K, Lu Z, Zhang K (2019) Multivariate output global sensitivity analysis using multi-output support vector regression. Structural and Multidisciplinary Optimization.

Dasari SK, Cheddad A, Andersson P (2020) Predictive modelling to support sensitivity analysis for robust design in aerospace engineering. Structural and Multidisciplinary Optimization, 61

Eamon CD, Rais-Rohani M (2008) Integrated reliability and sizing optimization of a large composite structure. Marine Structures, 22(2).

Ehre M, Papaioannou I, Straub D (2020) A framework for global reliability sensitivity analysis in the presence of multi-uncertainty. Reliability Engineering and System Safety, 195(C).

Faes M, Broggi M, Patelli E, Govers Y, Mottershead J, Beer M, Moens D (2019). A multivariate interval approach for inverse uncertainty quantification with limited experimental data. Mechanical Systems and Signal Processing, 118.

Faes M, Cerneels J, Vandepitte D, Moens D (2017) Identification and quantification of multivariate interval uncertainty in finite element models. Computer Methods in Applied Mechanics and Engineering, 315.

Fang SE, Zhang QH, Ren WX (2015) An interval model updating strategy using interval response surface models. Mechanical Systems and Signal Processing, 60-61.

Fujita K, Takewaki I (2011) An efficient methodology for robustness evaluation by advanced interval analysis using updated second-order Taylor series expansion. Engineering Structures, 33(12).

Ha S (2018) A local sensitivity analysis for the kinetic Cucker-Smale equation with random inputs. Journal of Differential Equations, 265(8).

Homma T, Saltelli A (1996) Importance measures in global sensitivity analysis of nonlinear models. Reliability Engineering and System Safety, 52(1).

Ishigami T, Homma T (1990) An importance quantification technique in uncertainty analysis for computer models.

Jacomel TA, André NA (2021) A priori error estimates for local reliability-based sensitivity analysis with Monte Carlo Simulation. Reliability Engineering and System Safety.

Khodaparast HH, Mottershead JE, Badcock KJ (2011) Interval model updating with irreducible uncertainty using the Kriging predictor. Mechanical Systems and Signal Processing, 25(4).

Kitahara M, Bi S, Broggi M, Beer M (2022) Nonparametric Bayesian stochastic model updating with hybrid uncertainties. Mechanical Systems and Signal Processing, 163, 108195.

Li D, Tang H, Xue S, Su Y (2018) Adaptive sub-interval perturbation-based computational strategy for epistemic uncertainty in structural dynamics with evidence theory. Probabilistic Engineering Mechanics, 53.

Liu Y, Liu Z, Zhong H, Qin H, Lv C (2019) Gauge sensitivity analysis and optimization of the modular automotive body with different loadings. Structural and Multidisciplinary Optimization, 60(1).

Tian LF, Lu ZZ, Hao WR (2012) Investigation of the uncertainty of the in-plane mechanical properties of composite laminates. Proceedings of the Institution of Mechanical Engineers, Part C: Journal of Mechanical Engineering Science, 226(7).

Lukáš N (2022) On distribution-based global sensitivity analysis by polynomial chaos expansion. Computers and Structures, 267.

Luo Z., Wang X., Liu D. (2020) Prediction on the static response of structures with large-scale uncertain-but-bounded parameters based on the adjoint sensitivity analysis. Structural and Multidisciplinary Optimization, 61(1).

Marrel A, Iooss B, Laurent B, Roustant O (2008) Calculations of Sobol indices for the Gaussian process metamodel. Reliability Engineering and System Safety, 94(3).

Mcrae GJ, Tilden JW, Seinfeld JH (1982) Global sensitivity analysis—a computational implementation of the Fourier Amplitude Sensitivity Test (FAST). Computers Chemical Engineering, 6(1), 15–25.

Moore RE (1966) Interval Analysis, Prentice-Hall.

Morris MD (1991) Factorial Sampling Plans for Preliminary Computational Experiments Technometrics, 33(2).

Papaioannou I, Straub D (2021) Variance-based reliability sensitivity analysis and the FORM α -factors. Reliability Engineering and System Safety, 210, 107496.

Liu QM, Dai YX, Wu XF, Han X, Ouyang H, Li ZR (2021) A non-probabilistic uncertainty analysis method based on ellipsoid possibility model and its applications in multi-field coupling systems. Computer Methods in Applied Mechanics and Engineering, 385.

Callens R, Faes M, Moens D (2022) MULTILEVEL QUASI-MONTE CARLO FOR INTERVAL ANALYSIS. International Journal for Uncertainty Quantification, 12(4).

Saltelli A, Tarantola S, Chan PS (1999) A Quantitative Model-Independent Method for Global Sensitivity Analysis of Model Output. Technometrics, 41(1), 39-56.

Shin MJ, Guillaume JHA, Croke BFW, Jakeman AJ (2013) Addressing ten questions about conceptual rainfall–runoff models with global sensitivity analyses in R. Journal of Hydrology, 503.

Singh R, Bhushan B (2020) Randomized algorithms for probabilistic analysis of parametric uncertainties with unmanned helicopters. Mechanical Systems and Signal Processing, 152.

Sobol IM (1993) Sensitivity estimates for nonlinear mathematical models. Math model comput exp 1(1), 112-118.

Sobol IM (2001) Global sensitivity indices for nonlinear mathematical models and their Monte Carlo estimates. Mathematics and Computers in Simulation (1). 55(1-3), 271-280.

Suzana E, Ivan D, Javier FJA (2022) Review of finite element model updating methods for structural applications. Structures, 41.

Wang C, Gao W, Yang CW, Song C (2011) Non-Deterministic Structural Response and Reliability Analysis Using a Hybrid Perturbation-Based Stochastic Finite Element and Quasi-Monte Carlo Method. Computers, Materials and Continua, 25(1), 19-46.

Wang C, Qiu ZP (2014). An interval perturbation method for exterior acoustic field prediction with uncertain-but-bounded parameters. Journal of Fluids and Structures, 49.

Wu Z, Wang D, Wang W, Zhao K, Zhou H, Zhang W (2020) Hybrid metamodel of radial basis function and polynomial chaos expansions with orthogonal constraints for global sensitivity analysis. Structural and Multidisciplinary Optimization.

Xiao NC, Huang HZ, Wang Z, Yu P, He L (2011). Reliability sensitivity analysis for structural systems in interval probability form. Structural & Multidisciplinary Optimization, 44(5), 691-705.

Zhang K, Lu Z, Cheng L, Xu F (2015) A new framework of variance based global sensitivity analysis for models with correlated inputs. Structural Safety, 55, 1-9.

Zhang, X., Deng, Z., & Zhao, Y. (2019). A frequency response model updating method based on unidirectional convolutional neural network. Mechanics of Advanced Materials and Structures, 28(14), 1-8.

Zhao YL, Deng ZM, Guo ZP (2018) Uncertainty static analysis of structures with hybrid spatial random and interval properties. Acta Mechanica.

Zhao YL, Deng ZM, Han YW (2019) Dynamic response analysis of structure with hybrid random and interval uncertainties. Chaos, Solitons and Fractals, 131.

Zhao YL, Yang JH, Faes M, Bi SF, Wang Y (2022) The sub-interval similarity: A general uncertainty quantification metric for both stochastic and interval model updating. Mechanical Systems and Signal Processing, 178.

Zhou C, Lu Z, Zhang L, Hu J (2014) Moment independent sensitivity analysis with correlations. Applied Mathematical Modelling, 38(19-20), 4885-4896.